ACTA CHEMICA SCANDINAVICA 14 (1960) 1961–1979

The Structures of Co_2P, Ru_2P and Related Phases

STIG RUNDQVIST

Institute of Chemistry, University of Uppsala, Uppsala, Sweden

The crystal structures of Co_2P and Ru_2P have been refined using single-crystal methods. Both phosphides crystallize in the *C* 23 structure type. A structural comparison with related phosphides and silicides is given.

Co_2P has an extended homogeneity range at higher temperatures, the phosphorus-rich limit at 1 000°C corresponds to the formula $Co_{1.94}P$. There are evidences that the widening of the homogeneity range is connected with random vacancies on metal atom sites.

The structure of Co_2P was originally determined by Nowotny [1]. According to him, the Co_2P structure belongs to the *C* 23 (anti-$PbCl_2$) type. The structure of Co_2Si was first investigated by Borén [2]. Borén *et al.*[3] also made a structure proposal based on X-ray powder data. This structure was later shown to be incorrect by Geller [4], who determined the Co_2Si structure by X-ray single-crystal methods. It was then recognized by Laves [5] that Co_2P and Co_2Si are isotypic, which was the first known case of isomorphism between a silicide and a phosphide of the same metal. Recently, a second case has been found for Ru_2P[6] and Ru_2Si[7], which are isostructural with Co_2P and Co_2Si.

From the crystal-chemical point of view it seems valuable to possess detailed structural information on the four above-mentioned phases. This paper gives an account of single-crystal structure determinations of Co_2P and Ru_2P. Some phase-analytical data for the binary Co_2P and Ru_2P, and the ternary $Co_2(P, Si)$ phases are also reported and discussed.

EXPERIMENTAL

Preparation. The starting materials for the preparation of the phosphides were cobalt rods (Johnson, Matthey & Co., Ltd., London, spectrographically standardized), ruthenium sponge (Heraeus, Hanau, Germany claimed purity 99.8 %) and red phosphorus (purity higher than 99 %). Master alloys of Co_2P were prepared according to a method, described in principle by Haughton [8] and Hägg [9]. Pellets of red phosphorus were dropped into molten cobalt. The melting was done by induction heating in a closed chamber in a purified argon atmosphere under reduced pressure. Cobalt phosphides of varying compositions were prepared by mixing appropriate quantities of the crushed master alloys and heating the mixtures in evacuated and sealed silica tubes. Ruthenium phosphides were prepared directly by heating ruthenium sponge and red phosphorus in evacuated silica tubes. The alloys of both cobalt and ruthenium were protected from contacting the silica tube walls by placing them in small crucibles of recrystallized alumina (Degussit Al 23 from Degussa, Frankfurt).

Chemical analyses. Chemical analyses were made at the Department of Analytical Chemistry of this Institute under the direction of the head of the department, Dr. F. Nydahl.

The cobalt phosphides were dissolved in *aqua regia*, and the hydrochloric acid removed by evaporation with nitric acid. The residue was dissolved in dilute nitric acid and made up to volume. Aliquots were analysed for phosphorus and cobalt. Phosphate was precipitated as ammonium molybdophosphate and weighed as $P_2O_5 \cdot 24\ MoO_3$ according to Nydahl [10]. Cobalt was determined by titration with EDTA, standardized against pure cobalt (cobalt rods, Johnson, Matthey & Co., Ltd.). Murexid was used as indicator and the pH adjusted with sodium carbonate in stead of ammonia to avoid formation of ammines [11].

The compositions of the ruthenium phosphides were checked by analyses for phosphorus only. The alloys were dissolved in hydrochloric acid — chlorine by heating in sealed glass tubes at 300°C for 24—48 h [12-15] (*cf.* [16]). Perchloric acid was used as oxidant for the evolution of chlorine. 1—2 g of sodium chloride was added to the solution, which was then evaporated to dryness to remove traces of silicic acid. The residue was taken up in hydrochloric acid and filtered. Ruthenium was removed by precipitation as the sulphide and phosphorus determined in the filtrate according to the method described above.

X-Ray methods. X-Ray powder photographs were taken using Guinier-type focussing cameras and Cr-$K\alpha_1$ and Cu-$K\alpha$ radiation ($\lambda_{\text{Cr-}K\alpha_1} = 2.2896$ Å; $\lambda_{\text{Cu-}K\alpha} = 1.5418$ Å). Calcium fluoride ($a = 5.4630$ Å) or silicon ($a = 5.4306$ Å) was used as the internal calibration standard on each powder film. Differences larger than 0.02 % for lattice parameters of the same phase, measured in different alloys, were estimated to be significant, whereas the absolute accuracy of a single lattice parameter measurement is not claimed to be greater than 0.04 %.

For the structure determinations, single-crystal fragments were picked from crushed alloys. Weissenberg photographs were taken with niobium-filtered Mo-*K* radiation. The multiple-film technique was used, and thin iron foil was placed between successive films. The intensities were estimated by visual comparison with a standard intensity scale. Since it was only possible to obtain single-crystals of rather irregular shape, absorption corrections could not be readily applied. However, care was taken to use small crystals (maximum thickness not exceeding 0.04 mm) with a fairly uniform cross-section, thus minimizing the influence of absorption as well as secondary extinction.

The refinement of the structures was made with the aid of the electronic digital computer BESK. The programs for Fourier summations and structure factor calculations are designed by Edstrand, Westman *et al.*[17] and Åsbrink *et al.*[18] For the atomic scattering factors f_i, analytical expressions of the type $f_i = A_i \exp\left(-\frac{a_i}{\lambda^2}\sin^2\Theta\right) + B_i \exp\left(-\frac{b_i}{\lambda^2}\sin^2\Theta\right) + C_i \exp\left(-\frac{c_i}{\lambda}\sin^2\Theta\right) + D_i$ were used. The constants A_i, B_i, C_i and a_i b_i, c_i, have been determined by Appel [19] on the basis of atomic scattering factor tables given by Thomas and Umeda [20] for Co and Ru, and by Tomiie and Stam [21] for P. The following constants were used:

	A_i	B_i	C_i	a_i	b_i	c_i
Co	9.319	10.181	7.273	0.328	3.556	25.673
Ru	15.176	16.599	11.760	0.240	2.637	20.292
P	1.447	7.971	5.588	0.001	1.528	37.194

In the case of Ru, a correction for dispersion was made by introducing the real part of the dispersion correction as the constant D_i in the above-mentioned expression for the scattering factors. This was taken as the value calculated by Dauben and Templeton [22].

PHASE-ANALYTICAL INVESTIGATIONS

In the binary system Co—P, three intermediate phases have been reported, *viz.* Co_2P, CoP and CoP_3, [23-25,1,26], and in the binary system Ru—P three phases Ru_2P, RuP and RuP_2 are known [27,6].

Nowotny [1] found that the unit cell dimensions of Co_2P are variable, indicating an extended homogeneity range. The present investigation shows that the unit cell of Co_2P decreases with decreasing cobalt content, which has also been verified by Nowotny [28]. The phase-analytical data are collected in Tables 1 and 2. On account of the difficulties of detecting small amounts of cobalt with the X-ray method, the cobalt-rich limit of the homogeneity range could not be accurately located. Judging from the lattice parameter measurements in Table 2, this limit is probably not far from the ideal composition Co_2P. The X-ray method is more sensitive for the detection of small amounts of CoP. The data in Tables 1 and 2 show that the phosphorus-rich limit at 1 000°C is very close to the composition $Co_{1.94}P$, and furthermore that the homogeneity range of Co_2P becomes larger when the temperature is increased from 900°C to 1 100°C.

No lattice parameter variations were found for Ru_2P in alloys with different compositions quenched from temperatures up to 1 100°C. The composi-

Table 1. Phase-analytical data for alloys containing Co_2P.

Alloy	Chemical analysis		Phases present in alloys quenched from		
	Weight % Co	Weight % P	900°C	1 000°C	1 100°C
$Co_{2.07}P$	79.57	20.20	Co_2P traces of Co	Co_2P traces of Co	Co_2P traces of Co
$Co_{1.94}P$	78.51	21.28	Co_2P traces of CoP	Co_2P	Co_2P
$Co_{1.89}P$	78.20	21.70	Co_2P traces of CoP	Co_2P traces of CoP	Co_2P traces of CoP

Table 2. Unit cell dimensions of Co_2P in Å measured on the alloys specified in Table 1.

Quenching temp. °C	Axis	$Co_{2.07}P$	$Co_{1.94}P$	$Co_{1.89}P$
900	a	5.646	5.640	5.641
	b	3.513	3.509	3.509
	c	6.608	6.605	6.605
1 000	a	5.646	5.638	5.638
	b	3.513	3.507	3.507
	c	6.608	6.603	6.603
1 100	a	5.646	5.638	5.634
	b	3.513	3.507	3.505
	c	6.608	6.603	6.601

tion of Ru_2P at 1 100°C was "bracketed" with two annealed and quenched alloys; one containing (besides Ru_2P) traces of ruthenium, and the other containing (besides Ru_2P) traces of RuP. Chemical analysis of the first alloy gave a phosphorus content of 13.20 wt % and the other 13.34 wt %. The phosphorus content calculated for the ideal composition Ru_2P is 13.29 wt %. Thus, at 1 100°C, the composition of Ru_2P is close to the ideal formula. (There is no reason to believe that the alloys take up any appreciable amount of impurities during the preparations.) The melting point of Ru_2P is much higher than that of Co_2P, and a widening of the homogeneity range of Ru_2P at temperatures above 1 100°C cannot be excluded. In fact, the structure determination made on a single-crystal picked from an arc-melted alloy, indicates such a possibility (*vide infra*).

THE REFINEMENT OF THE Co_2P STRUCTURE

In view of the phase-analytical results it was thought worthwhile to collect intensity data for two Co_2P single-crystals with different compositions. One crystal was selected from a cobalt-rich alloy sintered at 1 100°C. Since it proved very difficult to obtain phosphorus-rich single-crystals from alloys sintered in silica tubes, a very small single-crystal was finally taken from an alloy, melted in an argon-filled arc furnace and rapidly cooled. The composition of the alloy before melting was $Co_{1.89}P$, but some phosphorus was lost during the melting. The powder photograph of the arc-melted alloy gave the following lattice parameter values: $a = 5.638$ Å; $b = 3.507$ Å; $c = 6.603$ Å, corresponding to a composition around $Co_{1.94}P$. Since the diffraction lines were not as sharp as those of carefully annealed alloys, the arc-melted alloy may have been slightly inhomogeneous.

In the following text, the sintered crystal is denoted as Co_2P and the arc-melted crystal $Co_{1.94}P$. Weissenberg diagrams of both crystals were taken about the b axis.

According to Nowotny [1], the structure of Co_2P is based on space-group $Pnma$ — (D_{2h}^{16}), with eight cobalt atoms in two 4(c) positions and four phosphorus atoms in one 4(c) position *. If the space-group is $Pnma$, the reflexions (h00) with $h = 2n + 1$ are extinct. However, a weak (300) reflexion was observed for both crystals (although relatively weaker for the $Co_{1.94}P$ crystal than for the Co_2P crystal), and these spots on the photographic films were not significantly different in shape from the spots of other reflexions. It was nevertheless suspected that (300) might arise from double-reflexion. Calculations showed that the geometrical conditions for double-reflexion from ($\bar{2}\bar{1}\bar{1}$) and (511) were closely fulfilled. Furthermore, (211) and (511) were observed to be among the very strongest reflexions. It has been pointed out by Jellinek [29] that the effect of double-reflexion can be recognized in single-crystal photographs taken with unfiltered radiation. If the geometrical conditions for

* The C 23 structure has been described with different settings of the unit cell. Nowotny [1] (and *Strukturbericht*) used the space-group $P\ b\ n\ m$, and Geller [4] $P\ n\ a\ m$. In the present paper, the C 23 structure is always described on space-group $P\ n\ m\ a$, following the standard setting (No. 62) in the 1952 edition of *International Tables for X-ray Crystallography*.

double-reflexion are fulfilled for the $K\alpha$ radiation this will not hold for the $K\beta$ radiation. A special exposure with unfiltered MoK radiation was therefore made. β-reflexions corresponding to α-reflexions of equal or even lower intensity than (300), *e.g.* (400), were clearly seen but no β-reflexion corresponding to (300) was discernible. This was taken as definite evidence that (300) arises from double-reflexion.

All the remaining reflexions were consistent with space-group *Pnma* or $Pn2_1a$. Since the intensity sequences for the ($h0l$) and the ($h2l$) reflexions were equal, and the same was true for the ($h1l$) and ($h3l$) reflexions, it was not considered necessary to take the lower space-group $Pn\ 2_1a$ into account, and it was assumed that Nowotny's structure proposal was essentially correct. The signs of the $F(h0l)$-values were obtained from the atomic parameters given by Nowotny, and the electron density projections $\varrho(xz)$ were computed. All atoms are well resolved in this projection, and maxima appeared at the expected positions. The structures were refined with successive difference syntheses.

In the difference synthesis of the $Co_{1.94}P$ crystal, a distinct negative region of "electron density" was observed at the Co_{II} position, whereas the electron density was not very different from zero in other parts of the difference map, including the regions around the Co_I and P positions. No such phenomenon was observed in the difference maps for the Co_2P crystal. The minimum may originate from various sources. A closer analysis of the electron density maxima in the ϱ_{obs} and ϱ_{calc} projections showed that the effect must be ascribed to an incorrect scale factor for the Co_{II} atoms rather than an incorrect temperature factor. There were no definite indications that the temperature factors for Co_I, Co_{II} and P were very different or anisotropic. It was found that the minimum at the Co_{II} position was removed from the difference map, when an atomic scattering factor $f_{Co_{II}} = 0.96 \cdot f_{Co_I}$ was inserted in the structure factor calculations. The introduction of the lower scattering parameter for Co_{II} resulted in a decrease of the R-value for the 87 observed F-values from 0.060 to 0.053. An overall temperature factor with $B = 0.40$ Å^2 was applied.

$Co_{1.94}P$ presents a favourable case for scattering parameter comparison of the metal atoms from relative intensities only. Since the same kind of "heavy" atoms is compared in the same type of crystallographic position, the choice of scale factor between absolute and observed structure factors is not critical. However, the influence of absorption and extinction may not be negligible, and the question still remains whether the observed difference between the scattering parameters of Co_I and Co_{II} is significant or not. An attempt to study this problem was made in the following way.

A difference synthesis map for $Co_{1.94}P$, based on F_c-values computed with the atomic scattering factors $f_{Co_{II}} = 0.96 \cdot f_{Co_I}$, was prepared by calculating $\Delta\varrho$-values for every sixtieth x and z. The standard deviation $\sigma(\Delta\varrho) = \{\overline{(\Delta\varrho)^2}\}^{\frac{1}{2}}$ was calculated for the 900 independent $\Delta\varrho$-values. In the $\varrho_{obs}(xz)$ projection, the area around each cobalt position, in which the electron density values rose appreciably over the background, extended over some 30—40/3 600 of the projection. 35 $\Delta\varrho$-values for adjoining points in the difference map were summed over areas in various positions of the unit cell. The standard deviation of this sum is $\sqrt{35} \cdot \sigma(\Delta\varrho) = \sigma(N)$. The value of the sum in the area around an atomic position, gives a measure of the difference between the observed and calculated scattering parameter of the actual atom, and the sum is not very sensitive to errors in the assigned temperature factors. It was found that the numerical value of the sum never exceeded $4 \cdot \sigma(N)$ wherever the closed area was placed in the difference map.

Another difference map was calculated on the basis of equal scattering parameters for Co_I and Co_{II}. As mentioned before, this map contained a large minimum at the Co_{II} position; this minimum was not removed by omitting $F_o - F_c$ values for the strong reflexions, which shows that it cannot be ascribed to secondary extinction. When the sum over 35 $\Delta\varrho$-values was evaluated in the area around the Co_{II} position the numerical value of the sum was found to be 14 times larger than σ(N), whereas the sum did not exceed $4 \cdot \sigma$(N) in other areas of the difference map. This indicates that the difference between the scattering parameters of Co_I and Co_{II} is a significant effect. It is felt, however, that only a limited confidence can be attached to the actual numerical value of 1.1 electrons.

The interpretation of the difference is not obvious, and several explanations are possible. It will be shown later, however, that the assumption of random vacancies on the Co_{II} position leads to a satisfactory agreement with phase-analytical data and crystal chemical considerations. The final structural data obtained for the two crystals are the following:

Space-group $Pnma - (D_{2h}^{16})$, (No. 62)
All atoms in 4(c) positions.

The Co_2P crystal

a = 5.646 Å; b = 3.513 Å; c = 6.608 Å; U = 131.1 Å^3

	Atomic parameters and standard deviations				Scattering parameters (electrons)
	x	$\sigma(x)$	z	$\sigma(z)$	
Co_I	0.8560	0.0003_8	0.0647	0.0003_3	27.0
Co_{II}	0.9685	0.0003_8	0.6657	0.0003_3	27.0
P	0.2461	0.0007_8	0.1249	0.0006_7	15.0

The $Co_{1.94}P$ crystal

a = 5.638 Å; b = 3.507 Å; c = 6.603 Å; U = 130.6 Å^3

	Atomic parameters and standard deviations				Scattering parameters (electrons)
	x	$\sigma(x)$	z	$\sigma(z)$	
Co_I	0.8562	0.0003_3	0.0631	0.0002_8	27.0
Co_{II}	0.9684	0.0003_3	0.6664	0.0002_8	25.9
P	0.2437	0.0006_5	0.1232	0.0005_5	15.0

The standard deviations of the atomic parameters were estimated by Cruickshank's [30] formula. Observed and calculated structure factors for both crystals are collected in Table 3. For the Co_2P crystal (which was larger than the $Co_{1.94}P$ crystal) the R-value for the 104 observed reflexions is 0.088. An overall temperature factor with $B = 0.42$ Å^2 was applied.

Interatomic distances are listed in Table 4a and b. The standard deviations of the Co—Co distances are smaller than 0.004 Å; those of the Co—P distances smaller than 0.005 Å. (Errors in the unit cell dimensions have not been taken into account.) A comparison of corresponding interatomic distances in Co_2P and $Co_{1.94}P$ shows that the differences are very small.

Table 3. Calculated and observed F(*h*0*l*)-values for Co_2P, $Co_{1.94}P$ and Ru_2P.

		Co_2P		$Co_{1.94}P$		Ru_2P	
h	l	F_c	F_o	F_c	F_o	F_c	F_o
2	0	15.9	16.7	13.0	17.6	55.8	65.6
4	0	19.4	16.5	17.3	18.7	18.9	21.1
6	0	21.5	16.5	20.9	18.4	71.9	71.7
8	0	33.9	34.8	33.8	34.2	82.7	84.8
10	0	−40.5	41.2	−40.3	40.2	− 42.5	50.0
12	0	− 7.3		− 7.8		− 5.6	
14	0	− 3.6		− 2.3		11.5	
16	0					11.7	
1	1	7.8	10.4	10.9	10.9	10.0	7.2
2	1	− 2.8		− 2.2		− 29.0	31.3
3	1	−88.6	77.4	−88.6	90.8	−152.4	146.1
4	1	44.8	42.8	42.0	45.9	58.7	64.6
5	1	−20.3	16.6	−18.6	19.2	− 53.2	58.6
6	1	49.6	39.6	49.8	48.8	76.5	78.8
7	1	27.6	24.4	26.7	27.1	38.6	47.9
8	1	14.4		12.5		19.0	12.7
9	1	− 2.0		− 0.6		− 12.1	
10	1	16.3	14.9	16.9	16.8	25.6	24.3
11	1	−11.3	12.5	−13.0		− 35.2	38.9
12	1	14.7		13.6		37.4	37.4
13	1	16.1	19.0	16.9		20.0	
14	1	4.3		4.9		20.3	
15	1	13.4		12.6		7.3	
16	1					2.2	
0	2	17.8	13.3	21.2	20.0	38.6	35.6
1	2	−20.7	26.1	−19.2	21.9	− 62.0	61.8
2	2	−46.5	53.9	−46.6	48.0	− 69.2	73.7
3	2	−84.3	77.8	−82.7	83.6	−113.3	112.5
4	2	−53.9	52.4	−53.7	54.0	− 82.7	84.3
5	2	25.1	21.8	25.7	26.3	46.2	46.2
6	2	11.2	13.9	11.2	13.3	3.6	
7	2	−50.7	46.3	−49.0	47.6	− 63.6	65.4
8	2	12.2	9.2	13.1	16.3	16.2	11.6
9	2	−26.9	25.2	−26.5	24.0	− 66.0	70.9
10	2	− 9.8		−10.4		− 27.3	27.9
11	2	−14.9		−14.3		− 30.2	25.3
12	2	4.2		4.1		− 4.1	
13	2	6.1		6.1		4.7	
14	2	13.2	15.5	13.7	14.0	16.8	
15	2	−13.1	10.6	−12.5	13.6	− 30.9	24.2
16	2					3.5	
1	3	87.6	91.4	85.8	82.3	130.4	118.8
2	3	−60.1	64.1	−59.0	59.3	−105.9	98.2
3	3	32.7	33.1	30.1	32.1	73.9	74.8
4	3	21.6	17.9	19.4	20.1	41.4	40.9
5	3	20.2	16.8	17.6	17.6	53.6	54.4
6	3	31.1	32.9	32.1	31.7	70.0	77.2
7	3	20.2	19.3	22.2	23.7	47.8	49.4
8	3	−23.9	23.1	−25.5	25.2	− 36.9	41.0

Table 3. Cont.

9	3	−9.6		−10.8		11.2	
10	3	−5.3		−4.6		−12.7	
11	3	−14.3	14.0	−14.0		−3.0	
12	3	13.4	10.6	12.5		31.9	35.1
13	3	−9.3		−9.6		−4.4	
14	3	0.0		0.9		7.6	
15	3	−7.9		−6.9		−5.4	
16	3					−16.3	
0	4	−70.8	75.6	−65.9	63.0	−135.0	119.3
1	4	−39.5	41.6	−38.5	38.8	−62.5	58.1
2	4	2.6		4.0		−27.2	30.5
3	4	3.4		1.3		−23.2	22.1
4	4	−41.5	38.1	−42.0	40.8	−50.5	50.7
5	4	72.9	65.0	73.4	69.6	115.1	113.7
6	4	11.5	14.1	12.7	13.2	−20.4	24.2
7	4	25.4	24.7	24.4	25.2	33.9	37.2
8	4	−14.9	14.8	−13.9		−39.8	47.2
9	4	−2.9		−3.2		−10.1	
10	4	14.8		13.5		15.1	
11	4	21.3	19.8	20.8	20.0	34.0	32.3
12	4	−4.8		−3.9		−2.3	
13	4	15.3		15.9		41.6	35.8
14	4	8.7		8.7		3.2	
15	4	−6.8	8.7	−7.2		−2.2	
16	4					4.0	
1	5	−42.0	45.3	−40.9	40.8	−67.5	62.9
2	5	−65.5	65.7	−66.5	62.3	−92.1	85.5
3	5	2.0		0.9		34.5	33.0
4	5	−7.9		−5.5		−13.7	12.8
5	5	−8.8	11.1	−10.4		−4.2	
6	5	−6.8		−5.8		−6.1	
7	5	−14.1		−11.4		−44.3	46.6
8	5	−40.2	39.7	−38.9	39.1	−67.6	65.5
9	5	3.4		1.9		−2.0	
10	5	−23.8	25.0	−24.6	24.9	−50.3	56.6
11	5	12.5		13.1		23.6	26.5
12	5	5.4		7.0		−4.9	
13	5	0.0		−0.2		−9.8	
14	5	−5.3		−5.5		−17.6	
15	5	2.9		3.8		−5.5	
16	5					−23.4	
0	6	11.7	12.1	10.1	9.4	−13.2	
1	6	−50.9	51.4	−53.1	49.7	−45.8	42.7
2	6	52.0	52.2	51.6	47.7	101.6	95.4
3	6	12.8	12.0	11.2	10.9	18.5	16.0
4	6	55.0	52.1	51.5	48.1	111.0	103.5
5	6	4.5		5.6		17.1	16.7
6	6	−4.0		−2.5		11.8	
7	6	14.5	11.1	13.6		27.9	22.7
8	6	−11.1	10.2	−11.7		−16.4	
9	6	−22.4	23.1	−23.9	24.1	−13.8	
10	6	5.8		5.9		39.8	36.5
11	6	12.3		12.1		20.0	19.9
12	6	−8.5		−8.7		1.9	
13	6	1.4		2.1		9.7	

Table 3. Cont.

14	6	−16.6	17.0	−16.0	17.0	−25.0	22.7
15	6	−1.6		−2.4		3.1	
1	7	−47.6	45.2	−45.1	42.0	−106.9	101.3
2	7	1.0		−2.6		18.6	19.9
3	7	15.4	16.0	15.6	15.9	14.4	14.2
4	7	27.5	29.1	29.3	27.5	21.3	21.9
5	7	−2.2		−0.6		−18.1	
6	7	27.2	28.4	27.5	27.2	18.1	19.0
7	7	−28.5	31.2	−28.8	32.3	−71.3	75.0
8	7	15.2	13.6	14.9		30.0	28.2
9	7	9.0		9.4		−2.7	
10	7	10.2		8.7		20.1	
11	7	15.3	19.0	14.4		26.9	27.0
12	7	12.5		14.3		15.9	
13	7	−1.4		−1.1		−8.1	
14	7	2.1		1.4		9.8	
15	7					−6.6	
0	8	−34.3	35.0	−35.3	33.7	−49.8	51.2
1	8	−3.4		−7.2		7.6	
2	8	−26.3	26.8	−26.8	27.2	−12.9	
3	8	−15.3	12.2	−14.0	15.2	1.2	
4	8	34.5	36.1	34.7	34.9	56.1	59.0
5	8	−24.6	21.9	−22.6	24.4	−71.5	76.0
6	8	−34.6	34.5	−34.8	35.0	−41.1	44.8
7	8	−20.1	19.9	−18.4	18.3	−30.7	33.0
8	8	−2.1		−2.7		−16.6	
9	8	−14.0		−15.5		10.9	
10	8	11.1		11.9		16.7	14.1
11	8	−11.0		−9.6		−25.3	22.6
12	8	10.3		10.6		11.5	
13	8	−5.9		−5.4		−33.0	28.1
14	8	−8.3	7.5	−8.2		−18.5	16.8
15	8					−6.3	
1	9	14.6	12.6	12.9	11.9	34.1	33.6
2	9	16.3	16.5	13.8	15.9	57.4	58.7
3	9	47.4	47.4	47.4	44.2	71.7	72.3
4	9	−6.2		−6.5		−6.5	
5	9	19.4	20.0	20.3	19.4	42.8	47.3
6	9	−6.3		−5.4		−17.0	20.8
7	9	−15.7	19.5	−18.0	20.1	−3.3	
8	9	7.5		5.0		37.8	37.7
9	9	1.8		2.8		14.2	
10	9	4.8		4.5		26.1	25.7
11	9	1.4		1.5		12.4	
12	9	−6.0		−6.0		−9.3	
13	9	−17.3	12.4	−16.7	16.7	−8.3	
14	9					5.7	
0	10	−32.7	33.9	−32.0	32.9	−41.0	44.2
1	10	37.0	39.5	35.9	36.7	58.1	60.5
2	10	−10.1		−9.8		−52.8	54.8
3	10	7.4		6.9		22.7	23.6
4	10	3.7		7.9		−21.9	20.4
5	10	9.2		10.5		−19.4	23.0
6	10	−12.7		−14.5		−33.3	35.6

Table 3. Cont.

7	10	7.7		7.8		6.3	
8	10	−5.8		−6.0		−9.5	
9	10	38.0	30.8	36.4	32.7	51.7	57.0
10	10	10.6		11.0		−7.7	
11	10	−1.1		−0.5		0.0	
12	10	5.0		5.4		5.1	
13	10	2.1		2.1		−3.2	
14	10					2.5	
1	11	−14.4	14.0	−16.9	15.2	12.7	
2	11	14.7	13.3	15.0	14.5	30.8	33.3
3	11	−2.8		−0.8		−13.3	
4	11	−24.3	23.7	−24.0	22.3	−40.0	43.9
5	11	−4.8		−5.1		−2.8	
6	11	−28.4	29.4	−27.0	29.7	−54.3	59.6
7	11	−4.6		−6.2		13.3	
8	11	−4.3		−5.7		−7.5	
9	11	1.3		1.5		−1.2	
10	11	−4.9		−3.7		−11.3	
11	11	5.8		7.5		−7.8	
12	11	−17.7	15.8	−17.9	19.4	−39.7	34.5
13	11					3.4	
0	12	14.6	14.1	11.5		59.9	66.5
1	12	17.0	17.4	18.6	17.4	34.3	36.6
2	12	28.5	28.3	28.7	28.2	34.3	37.5
3	12	9.0		7.5		13.5	
4	12	1.8		3.5		−5.2	
5	12	−16.3	21.7	−16.7		−3.0	
6	12	15.3	14.8	13.8		38.8	40.7
7	12	1.8		−0.8		8.0	
8	12	−4.5		−5.4		17.2	
9	12	12.8	16.8	13.4	18.3	35.8	35.4
10	12	−2.0		−0.9		−8.6	
11	12	−6.2		−7.2		4.1	
12	12	−9.5		−9.3		−8.2	
13	12					2.6	
1	13	−4.3		−4.6		−13.1	
2	13	20.5	22.6	22.0	21.7	13.7	
3	13	−16.7	14.0	−13.8		−60.8	66.3
4	13	3.9		3.7		3.2	
5	13	−7.2		−6.9		−33.0	33.4
6	13	1.1		0.1		2.3	
7	13	6.6		6.0		13.4	
8	13	19.5	20.4	20.9	23.6	14.0	
9	13	−1.1		−1.4		−11.8	
10	12	18.0		18.0		11.3	
11	13	−0.7		0.4		−16.9	15.4
12	13					2.3	
0	14	6.6		3.6		32.1	40.0
1	14	−2.8		−1.1		−13.9	
2	14	−9.4		−8.8		6.3	
3	14	15.6		15.8		−11.9	
4	14	−15.5	17.0	−16.3	18.3	−28.2	31.0
5	14	−24.1	26.5	−25.5	31.1	−21.1	
6	14	5.1		5.1		24.3	24.7

Table 3. Cont.

7	14	−5.8		−5.4		−18.3	
8	14	5.3		4.4		13.2	
9	14	−9.4		−6.6		−27.2	21.1
10	14	−5.4		−4.2		−12.3	
11	14					−15.2	
1	15	22.8	22.5	22.6	27.4	37.0	36.9
2	15	2.8		4.4		−12.0	
3	15	−1.2		−1.3		0.5	
4	15	0.1		−1.1		17.2	
5	15	4.9		4.9		9.8	
6	15	−1.1		−3.6		24.2	21.1
7	15	11.9	10.8	11.7	11.4	28.0	25.2
8	15	3.5		4.7		5.5	
9	15	−3.8		−3.6		2.3	
10	15					6.5	
0	16	9.9		11.4		−14.0	
1	16	−0.2		0.6		−22.3	25.6
2	16	−14.1	14.6	−13.6	11.9	−30.6	31.3
3	16	4.4		6.2		−2.6	
4	16	−10.1		−10.2		−29.2	26.1
5	16	9.6		7.5		18.9	19.8
6	16	4.0		4.7		−11.9	
7	16	7.8		8.8		9.1	
8	16	8.0		8.4		−2.0	
9	16					−13.8	
1	17	1.1		1.3		8.4	
2	17	−9.6		−8.1		−28.3	27.6
3	17	−11.2	14.3	−11.0		7.3	
4	17	−5.3		−5.8		−3.1	
5	17	−3.4		−3.7		6.4	
6	17	−3.2		−3.7		0.0	
7	17					3.0	
8	17					−27.5	
0	18	14.7	19.8	17.1	18.6	9.2	
1	18	−2.8		−2.3		−10.1	
2	18	7.3		6.3		11.3	
3	18	−5.9		6.1		−1.6	
4	18					22.4	19.6
5	18					26.1	19.9
6	18					0.6	
1	19					−29.1	19.5
2	19					−9.3	
3	19					−6.6	

THE REFINEMENT OF THE Ru_2P STRUCTURE

Since it was virtually impossible to obtain single-crystals of Ru_2P in alloys sintered in silica tubes, single-crystal fragments were picked from an arc-melted alloy. Within experimental error the lattice parameters of Ru_2P in this alloy were equal to those measured in carefully annealed alloys. How-

Table 4a. Interatomic distances in Co_2P (Å). (Distances shorter than 3.3 Å listed).

	Co_I	Co_{II}	P
Co_I	$2.54_3(2)$	$2.62_4(2)$, 2.66_5 $2.69_1(2)$, 2.71_2	2.14, 2.23(2) 2.24
Co_{II}	$2.62_4(2)$, 2.66_5 $2.69_1(2)$, 2.71_2	$2.83_0(2)$ $3.03_5(2)$	2.29, 2.40(2) 2.54(2)
P	2.14, 2.23(2) 2.24	2.29, 2.40(2) 2.54(2)	3.27(2)

Table 4b. Interatomic distances in $Co_{1.94}P$ (Å). (Distances shorter than 3.3 Å listed).

	Co_I	Co_{II}	P
Co_I	$2.53_0(2)$	$2.62_5(2)$, 2.66_0 $2.69_1(2)$, 2.69_5	2.17, 2.21(2) 2.22
Co_{II}	$2.62_5(2)$, 2.66_0 $2.69_1(2)$, 2.69_5	$2.83_4(2)$ $3.02_7(2)$	2.29, 2.41(2) 2.54(2)
P	2.17, 2.21(2) 2.22	2.29, 2.41(2) 2.54(2)	3.28(2)

ever, the powder diffraction lines of the arc-melted alloy were not very sharp and the experimental error was therefore rather large (about 0.1 %). A widening of the homogeneity range of Ru_2P at higher temperatures (in analogy to Co_2P) cannot be excluded.

The Weissenberg photographs showed that Ru_2P is isostructural with Co_2P. The $\varrho(xz)$ projection was refined in a similar way to that described for Co_2P. It was observed in the difference syntheses of Ru_2P that there was a strong minimum of electron density at the Ru_{II} position as for $Co_{1.94}P$. Furthermore, an anisotropic temperature factor for Ru_{II} was indicated. The axes of the projected vibration ellipsoid for Ru_{II} happened to coincide rather closely to the directions of the crystallographic axes, and therefore, an anisotropic temperature factor of the simple form exp — $(\alpha h^2 + \gamma l^2)$ was applied.

The absorption was stronger in the Ru_2P crystal than in the Co_2P crystals, but it seems improbable that absorption errors would accumulate in such a way that a strong minimum of electron density is created at the Ru_{II} position, leaving the remaining part of the difference map, especially the vicinity of the Ru_I position, almost unaffected. After lowering the scattering parameter of Ru_{II} by 5.9 %, the resulting difference synthesis was free from large maxima and minima. A significance test, made in the way described earlier, yielded a similar result to that obtained for $Co_{1.94}P$.

The final structural data of the Ru_2P crystal are as follows:

Space-group *Pnma* — (D_{2h}^{16}) No. 62.
All atoms in 4(*c*) positions.

	Atomic parameters and standard deviations				Scattering parameters
	x	$\sigma(x)$	z	$\sigma(z)$	(electrons)
Ru_I	0.8585	0.0003_0	0.0736	0.0002_6	44.0
Ru_{II}	0.9780	0.0003_3	0.6586	0.0002_9	41.4
P	0.2455	0.0009_5	0.1135	0.0008_1	15.0

The standard deviations were estimated by Cruickshank's [30] formula. Observed and calculated structure factors are given in Table 3. For Ru_I and P, isotropic temperature factors with $B_{Ru_I} = 0.30$ Å^2 and $B_P = 0.40$ Å^2 were applied, whereas for Ru_{II} the anisotropic temperature factor, exp—$(0.00265\ h^2 + 0.00120\ l^2)$, was applied. The *R*-value for the 124 observed reflexions is 0.073.

Table 5. Interatomic distances in Ru_2P (Å). (Distances shorter than 3.5 Å listed).

	Ru_I	Ru_{II}	P
Ru_I	$2.74_6(2)$	2.75_8, $2.83_0(2)$ $2.84_0(2)$, 2.94_7	2.26, 2.30 2.40(2)
Ru_{II}	2.75_8, $2.83_0(2)$ $2.84_0(2)$, 2.94_7	$2.92_8(2)$ $3.20_9(2)$	2.32, 2.55(2) 2.82(2)
P	2.26, 2.30 2.40(2)	2.32, 2.55(2) 2.82(2)	

Interatomic distances calculated on the basis of the unit cell dimensions $a = 5.902$ Å; $b = 3.859$ Å; $c = 6.896$ Å; (obtained from powder photographs of carefully annealed alloys) are given in Table 5. The standard deviations for the Ru—Ru distances are smaller than 0.004 Å; those for the Ru—P distances smaller than 0.006 Å.

DESCRIPTIONS OF THE Co_2P AND Ru_2P STRUCTURES COMPARISONS WITH RELATED STRUCTURES

A projection of the Co_2P structure on the *ac* plane is shown in Fig. 1. The phosphorus atoms are situated in triangular prismatic "holes" in the metal atom lattice, with six metal atoms in the corners of the prism, and three metal atoms outside each rectangular side of the prism forming a triangle around the phosphorus atoms. The environment of the phosphorus atoms is shown for Co_2P in Fig. 2, and for Ru_2P in Fig. 3. These phosphides have their type of non-metal atom coordination in common with many other transition metal phosphides as well as with several transition metal borides, silicides and carbides. A study of the coordination of the phosphorus atoms around the metal

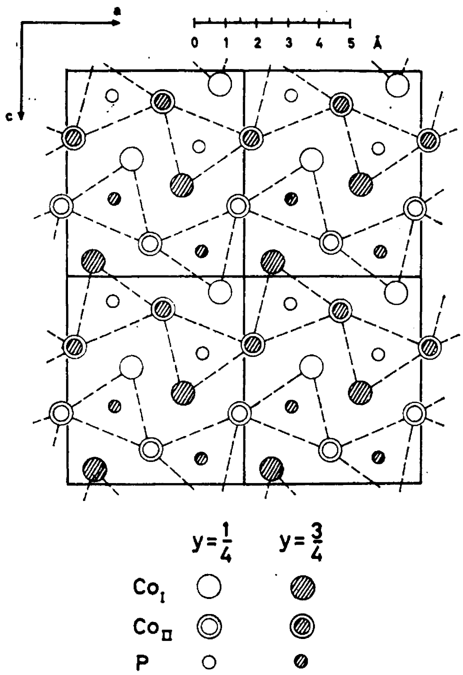

Fig. 1. The structure of Co_2P projected on (010).

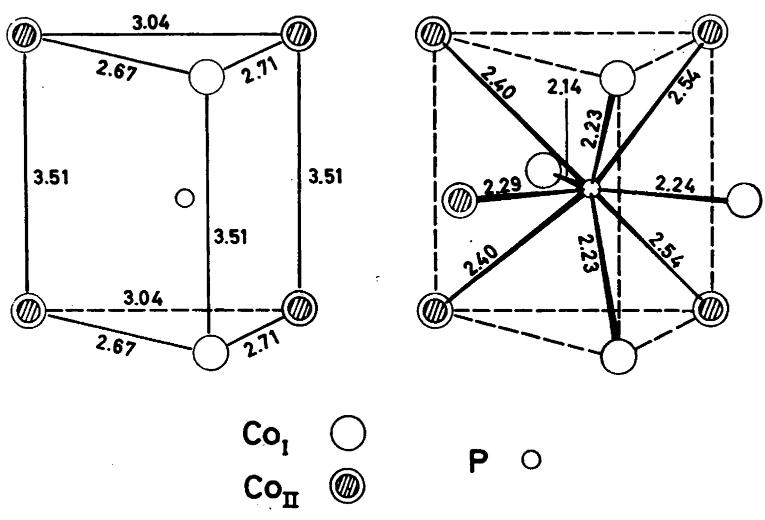

Fig. 2. The environment of the phosphorus atoms in Co_2P.

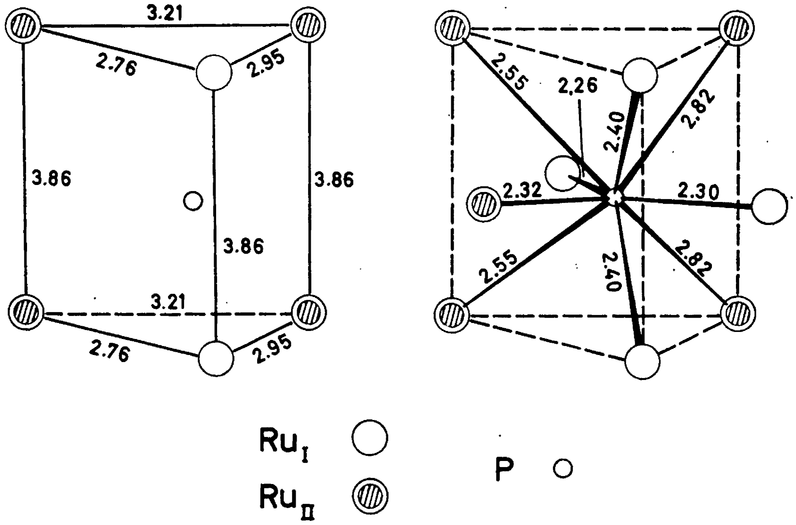

Fig. 3. The environment of the phosphorus atoms in Ru_2P.

atoms shows that Co_I and Ru_I have four phosphorus neighbours arranged in a slightly deformed tetrahedral configuration. The mean value of the Co_I—P distances is 2.21 Å and the mean of the Ru_I—P distances is 2.34 Å. These values are considerably smaller than the average Co_{II}—P and Ru_{II}—P distances. Co_{II} and Ru_{II} have five phosphorus neighbours with a mean Co_{II}—P distance of 2.44 Å and a mean Ru_{II}—P distance of 2.61 Å.

Besides Co_2P and Ru_2P, the structures of the following Me_2P phosphides (Me = transition metal) have been reported; *viz.* Mn_2P, Fe_2P and Ni_2P, which belong to the (revised) *C* 22 structure type [28], and Rh_2P and Ir_2P, which crystallize in the *C* 1 (anti-fluorite) structure [31,6].

The Co_2P and Ru_2P structures bear many resemblances to the *C* 22 type. A projection of the hexagonal Fe_2P structure on the basal plane is shown in Fig. 4. The coordination around the phosphorus atoms in Fe_2P is closely similar to the coordination of the phosphorus atoms in Co_2P. The Fe_I atoms have four phosphorus neighbours in a slightly distorted tetrahedral arrangement (average Fe_I—P distance 2.26 Å) and the Fe_{II} atoms have five phosphorus neighbours (average Fe_{II}—P distance 2.46 Å).

In Rh_2P and Ir_2P, all metal atoms have tetrahedral phosphorus coordination with the Rh—P distance 2.381 Å and the Ir—P distance 2.400 Å.

It was mentioned earlier in this paper that the structures of Co_2P and Co_2Si as well as those of Ru_2P and Ru_2Si are isotypic. A detailed comparison of Co_2P and Co_2Si, however, reveals distinct differences. The situation is quite analogous for Ru_2P and Ru_2Si.

A projection of the Co_2Si structure on the *ac*-plane (according to Geller [4]) is shown in Fig. 5. The near environment of the silicon atoms consists of ten cobalt atoms at distances between 2.32 and 2.57 Å. (An eleventh cobalt atom is

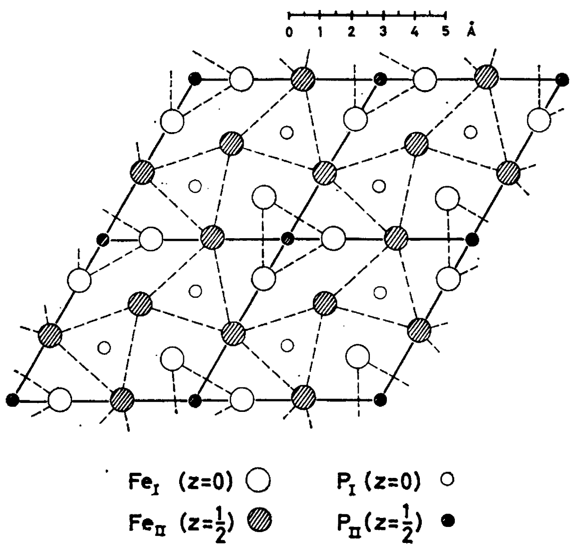

Fig. 4. The structure of Fe_2P projected on (001).

situated at a distance of 3.25 Å and four silicon atoms at a distance of 3.15 Å). In Co_2P, the phosphorus atoms have only nine close cobalt contacts with P—Co distances between 2.14 and 2.55 Å. (Two additional cobalt atoms are situated at distances of 3.42 Å and 3.47 Å, and two phosphorus atoms at a distance of 3.27 Å.) As pointed out before, the coordination of the Co_I atoms in Co_2P is markedly different from that of the Co_{II} atoms. The situation is not analogous in Co_2Si, where the two sets of cobalt atoms each have eight cobalt neighbours and five silicon neighbours:

Co_I —8Co, average distance 2.63 Å; Co_I —5Si, average distance 2.39 Å
Co_{II}—8Co, average distance 2.59 Å; Co_{II}—5Si, average distance 2.46 Å

The unit cell volume of Co_2P is 131.1 Å^3 and the volume of Co_2Si is 130.7 Å^3. The two unit cells are, however, rather different in shape. The *b* and *c* axes in Co_2Si are larger than the corresponding axes in Co_2P, but the reverse is true for the *a* axis. There exists a limited mutual solid solubility between Co_2P and Co_2Si. The changes of the unit cell dimensions of Co_2P and Co_2Si, when these phases dissolve silicon and phosphorus respectively, are seen in Table 6, where lattice parameter measurements have been collected from two-phase $Co_2P + Co_2Si$ alloys, quenched from various temperatures. As seen in Table 6, the mutual solid solubility increases with increasing temperature. Data obtained with the "disappearing phase" method indicated that neither the solid solubility of Co_2P in Co_2Si, nor the solid solubility of Co_2Si in Co_2P exceeds 15 % in the investigated temperature range. In view of the differences between the structures of Co_2P and Co_2Si, it is not surprising that the mutual solid solubility is restricted, although the size-factor is favourable.

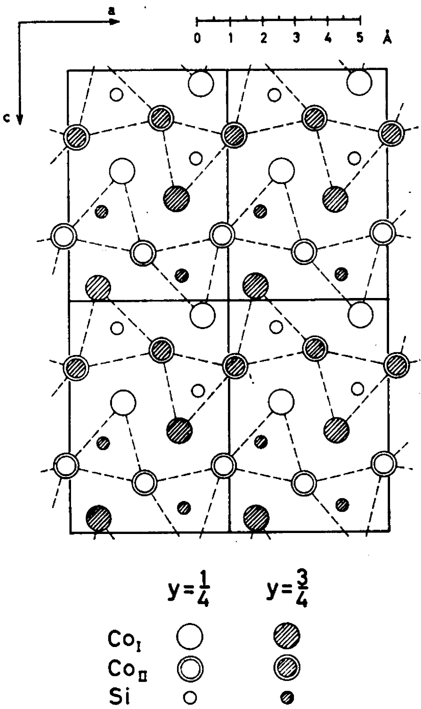

Fig. 5. The structure of Co_2Si projected on (010).

THE HOMOGENEITY RANGE OF Co_2P

The *C* 23 type of structure is rather close-packed, and the "holes" in the structure are not large enough for accomodation of additional atoms without profound distortion of the structure. The extended homogeneity range of Co_2P, (and probably of Ru_2P too), must therefore arise either from metal/phosphorus substitution or from vacant metal atoms sites (or possibly a combination of substitution and vacancies). This is also evident from the decrease of the Co_2P unit cell with increasing P/Co ratio.

The structure determinations on Co_2P and Ru_2P show that there are conspicuous differences between the Co_I and Ru_I atoms on one hand, and the Co_{II} and Ru_{II} atoms on the other. The coordination around the Co_I and Ru_I atoms is different from that of the Co_{II} and Ru_{II} atoms, and furthermore the electron counts indicate a lower scattering parameter for Co_{II} than for Co_I in the $Co_{1.94}P$ crystal (and analogously in the Ru_2P crystal).

The scattering parameter fo Co_{II} in the $Co_{1.94}P$ crystal was observed to be 1.1 electrons less than that of Co_I. If the scattering parameter difference is entirely ascribed to Co_{II}/P substitution, the calculated composition of the crystal is $Co_{1.75}P$, which is not compatible with the phase-analytical results. If the possibility of simultaneous vacancies on the P position is taken into account, the calculated composition of the crystal may be brought to a more

Table 6. Lattice parameters of Co_2P-Co_2Si mixed crystals. (Measurements made on a two-phase alloy with the composition $Co_2P_{0.5}Si_{0.5}$, quenched from various temperatures).

Quenching temp. °C	Phase	Lattice parameters (Å)		
		a	*b*	*c*
—	Co_2P	5.646	3.513	6.608
—	Co_2Si	4.918	3.737	7.109
1 000	$Co_2P(Si)$	5.607	3.537	6.644
	$Co_2Si(P)$	4.954	3.719	7.065
1 075	$Co_2P(Si)$	5.600	3.540	6.650
	$Co_2Si(P)$	4.965	3.715	7.048
1 150	$Co_2P(Si)$	5.595	3.543	6.654
	$Co_2Si(P)$	4.982	3.709	7.039

reasonable value, but this idea seems far-fetched and it is not supported by the data of the structure determination. On the other hand, if the lowering of the Co_{II} scattering parameter is ascribed only to random vacancies among the Co_{II} atoms, the composition of the crystal should be $Co_{1.96}P$, which is in fairly good agreement with the phase-analytical data. This supports the hypothesis of metal atom vacancies. It must be remembered, however, that it is possible to interpret the observed difference between the scattering parameters of Co_I and Co_{II} in other ways than those mentioned here.

Although the existence of metal/phosphorus substitution has been recognized in transition metals, *e.g.* in α-iron [32], the conditions for metal/phosphorus substitution in Co_2P and Ru_2P are probably less favourable. In the structures of transition metal phosphides with phosphorus contents of 50 atom per cent or less, P—P distances shorter than 3.0 Å have not been observed [33,34,26,28,35] Considering that metal/phosphorus substitution in Co_2P or Ru_2P would imply P—P distances shorter than 2.4 Å, the hypothesis of metal/phosphorus substitution in these phases appears less attractive. However, vacancies on transition metal sites has been found in phases similar to Ru_2P and Co_2P, *e.g.* in many phases belonging to the NiAs structure family.

Since strong arguments in favour of the hypothesis of metal/phosphorus substitution are lacking, it seems most reasonable to assume that the extended homogeneity range of Co_2P is connected with vacancies on cobalt atom sites.

One might ask if an analogous phenomenon exists in phosphides of the Fe_2P type. As mentioned earlier, the Fe_2P structure closely resembles the Co_2P structure. Unfortunately, accurate phase-analytical data are not available for any of the Fe_2P type phosphides, but a qualitative observation by Haughton [8] indicates an extended homogeneity range of Fe_2P. In his metallographic investigation of iron phosphides, Haughton found signs of secondary precipitation of FeP in the Fe_2P phase. His equilibrium diagram of the Fe—P system therefore contains a (dotted) line, which extends the Fe_2P single-phase field at higher temperatures towards the phosphorus-rich side of the diagram.

Acknowledgements: This work has been financially supported by the *Swedish State Council of Technical Research* and by the *Air Force Office of Scientific Research of the Air Research and Development Command, United States Air Force,* through its European Office under contract No. AF 61(052)—40. Facilities for use of the electronic digital computer BESK were given by the *Swedish Board for Computing Machinery.*

The author wishes to express his gratitude to Professor G. Hägg for his kind interest and valuable comments on the manuscript. Thanks are also due Dr. F. Nydahl and Dr. L. Gustafsson for their careful work on the chemical analyses. The author is much indebted to Mr. K. Nordgren, who collected the intensity material for the Co_2P crystal and made preliminary lattice parameter measurements on Co—P and Co—P—Si alloys, and also wishes to thank Dr. B. Aronsson and Dr. R. Hesse for many stimulating discussions.

REFERENCES

1. Nowotny, H. *Z. anorg. Chem.* **254** (1947) 31.
2. Borén, B. *Arkiv Kemi, Mineral. Geol.* **11 A** (1933) No. 10.
3. Borén, B., Ståhl, S. and Westgren, A. *Z. physik. Chem.* **B 29** (1935) 231.
4. Geller, S. *Acta Cryst.* **8** (1955) 83.
5. Laves, F. in Smithells, C. J. *Metals Reference Book,* 2nd ed. London 1955, p. 221.
6. Rundqvist, S. *Nature* **185** (1960) 31.
7. Aronsson, B., Åselius, J. and Stenberg, E. *Nature* **183** (1959) 1318.
8. Haughton, J. L. *J. Iron Steel Inst.* **115** (1927) 417.
9. Hägg, G. *Nova Acta Regiae Soc. Sci. Upsaliensis,* Ser. IV, **7** (1929) No. 1.
10. Nydahl, F. *Lantbrukshögsk. Ann.* **10** (1942) 114.
11. Nydahl, F. *Unpublished.*
12. Gordon, C. L. *J. Research NBS* **30** (1943) 107.
13. Wickers, E., Schlecht, W. G. and Gordon, C. L. *Ibid.* **33** (1944) 363.
14. Wickers, E., Schlecht, W. G. and Gordon, C. L. *Ibid.* **33** (1944) 451.
15 Gordon, C L., Schlecht, W. G. and Wickers, E. *Ibid.* **33** (1944) 457.
16. Hillebrand, W. F., Lundell, G. E. F., Bright, H. A. and Hoffman, J. I. *Applied Inorganic Analysis,* 2nd ed. New York 1953.
17. Westman, S., Blomqvist, G. and Åsbrink, S. *Arkiv Kemi* **14** (1959) 535.
18. Åsbrink, S., Blomqvist, G. and Westman, S. *Ibid.* **14** (1959) 545.
19. Appel, K. *Technical Note from the Quantum Chemistry Group, University of Uppsala.*
20. Thomas, L. H. and Umeda, K. *J. Chem. Phys.* **26** (1957) 293.
21. Tomiie, Y. and Stam, C. H. *Acta Cryst.* **11** (1958) 126.
22. Dauben, C. H. and Templeton, D. H. *Ibid.* **8** (1955) 841.
23. Żemcźużny, S. and Schepelew, J. *Z. anorg. Chem.* **64** (1909) 245.
24. Biltz, W., Heimbrecht, M. and Meisel, K. *Ibid.* **241** (1939) 349.
25. Fylking, K.-E. *Arkiv Kemi Mineral. Geol.* **11 B** (1935) No. 48.
26. Rundqvist, S. and Larsson, E. *Acta Chem. Scand.* **13** (1959) 551.
27. Biltz, W., Ehrhorn, H. J. and Meisel, K. *Z. anorg. Chem.* **240** (1939) 117.
28. Rundqvist, S. and Jellinek, F. *Acta Chem. Scand.* **13** (1959) 431 (*footnote*).
29. Jellinek, F. *Acta Cryst.* **11** (1958) 677.
30. Cruickshank, D. W. J. *Ibid.* **2** (1949) 65.
31. Zumbusch, M. *Z. anorg. Chem.* **243** (1940) 322.
32. Gale, B. *Acta Met.* **7** (1959) 420.
33. Schönberg, N. *Acta Chem. Scand.* **8** (1954) 226.
34. Aronsson, B. *Ibid.* **9** (1955) 137.
35. Rundqvist, S. and Hede, A. *Ibid.* **14** (1960) 893.